Neuromuscular Disorders

FULL LENGTH ARTICLE | VOLUME 30, ISSUE 11, P877-887, NOVEMBER 01, 2020

# The importance of an integrated genotype-phenotype strategy to unravel the molecular bases of titinopathies

Aurélien Perrin [1] • Raul Juntas Morales [1] • François Rivier • ... Valérie Rigau • Michel Koenig • Mireille Cossée • Show all authors • Show footnotes

Open Access • Published: September 28, 2020 • DOI: https://doi.org/10.1016/j.nmd.2020.09.032 •



## Highlights

- *TTN* variants are frequent and their pathogenicity is difficult to assess.
- Deep phenotyping, segregation studies, transcripts and protein analyses are essential.
- Analysis of the consequences on transcripts and protein of all variants is crucial.
- RNASeq will be the technique of choice to identify *TTN* variants consequences.
- Reporting challenging titinopathy cases in publications is essential.

## Abstract

Next generation sequencing (NGS) has allowed the titin gene (*TTN*) to be identified as a major

the phenotypic variability and the dominant or recessive pattern of inheritance are unclear. Titin is involved in the formation and stability of the sarcomeres. The effects of the different *TTN* variants can be harmless or pathogenic (recessive or dominant) but the interpretation is tricky because the current bioinformatics tools can not predict their functional impact effectively. Moreover, *TTN* variants are very frequent in the general population. The combination of deep phenotyping associated with RNA molecular analyses, western blot (WB) and functional studies is often essential for the interpretation of genetic variants in patients suspected of titinopathy. In line with the current guidelines and suggestions, we implemented for patients with skeletal myopathy and with potentially disease causing *TTN* variant(s) an integrated genotype-transcripts-protein-phenotype approach, associated with phenotype and variants segregation studies in relatives and confrontation with published data on titinopathies to evaluate pathogenic effects of *TTN* variants (even truncating ones) on titin transcripts, amount, size and functionality. We illustrate this integrated approach in four patients with recessive congenital myopathy.

## Keywords

Titinopathy • Congenital myopathy • Deep phenotyping • Titin transcripts • Titin western-blot

## 1. Introduction

*TTN* encodes titin, a giant sarcomeric protein [[1]] that plays important functional and structural roles in the sarcomere. Mutations in *TTN* are associated with a broad range of skeletal and/or cardiac phenotypes with autosomal dominant or recessive inheritance. Since the widespread use of Next Generation Sequencing (NGS), the exhaustive analysis of the 364 coding exons of *TTN* revealed an increasing number of reported *TTN* variants. Nevertheless, assessing the pathogenicity of the identified variants, in particular missense ones, is often difficult, due to the clinical heterogeneity of the pathology, the large size of the gene, the frequency of *TTN* variants in the general population (including 0, 36% of truncating variants affecting all transcripts [[2]]) and the complexity of gene expression (many different isoforms are expressed over time and tissue location) [[3]]. Different types of mutation have been reported as pathogenic, but their consequences on transcripts and protein, in particular loss or gain of titin function, are not fully elucidated. In myopathic titinopathies, several studies demonstrated that *TTN* truncating mutations are associated with loss function

(such as the titin kinase domain) and interaction domains (with proteins such as calpain-3, actin, myosin, nebulin, or one of the numerous interacting proteins (for review, see [[4]])) may suggest a potential pathogenicity. Specific variants in the last exon (including missense variants) and all the truncating variants causing the loss of the C-terminal portion (i.e. M-band truncating variants) causes the loss of the interaction with calpain-3 and its reduction at western blot, may contribute to disease pathogenesis, raising the possibility that the decrease of calpain-3 level may contribute to disease pathogenesis [5, 6, 7, 8, 9].

Expert laboratories have worked on the establishment of specific recommendations for *TTN* variants interpretation [[10]], based on familial and genetic data (number and type of variant(s)), histopathology [[11]], magnetic resonance imaging (MRI) [[12]] or clinical features [[13]]. In line with the current guidelines and suggestions [[2],[3],[14] the combination of deep phenotyping associated with RNA molecular analyses, western blot (WB) and functional studies is often essential for the interpretation of genetic variants in patients suspected of titinopathy. Namely, pattern featuring a prominent semi-tendinous muscle involvement on MRI, prominent nuclear internalization, peculiar alteration of oxidative reactions (such as cores, minicores and inverted cores) and presence of cytoplasmic bodies on muscle biopsy are suggestive and common, although non-specific, features found in all titinopathies.

For these reasons, we implemented a workflow based on deep phenotyping, comprehensive *TTN* variants assessment including bioinformatic predictions and evaluation of their effects on skeletal muscle titin transcripts and protein. We hereby describe our strategy for *TTN* variant interpretation in four patients with recessive congenital myopathy.

# 2. Methods

## 2.1 Patients

The study was approved by the ethical guidelines issued by our institutions for clinical studies in compliance with the Helsinki Declaration. Patients or parents gave informed consent for the genetic analysis according to French legislation (Comité de Protection des Personnes OUEST 6-CPP1128HPS3 IDRCB-2018-AO2287-48).

## 2.2 Bioinformatic evaluation of *TTN* Variants Pathogenicity

The pathogenicity of variants was assessed through a set of criteria reported by Zenagui et al.[[15]], according to the American College of Medical Genetics and Genomics (ACMG) guidelines [[16]]. In the present work, additional tools recently described were used: the MPA software [[17]] that aggregates bioinformatic prediction tools and provides a 0–10 prioritization score, accessible from https://mobidetails.iurc.montp.inserm.fr/, and the TITINdb, a database that takes into account several statistical and structural criteria for the interpretation of *TTN* variants (http://fraternalilab.kcl.ac.uk/TITINdb/) [[18]]. In addition, to take into account the complexity of skeletal transcripts of *TTN,* in particular the fact that some exons are only expressed during fetal development ("metatranscript-only exons"), we systematically referred to the recent study reported by Savarese et al. [[19]]. All variants presented in this study have been submitted in Leiden Open Variation Database (LOVD) https://databases.lovd.nl/shared/genes/TTN.

## 2.3 Muscle morphological analyses and immunohistochemistry

Open muscle biopsies were performed, frozen and fixed following previously described standardized methods and analyzed with histochemical, histoenzymatic, techniques with light and electron microscopy [[11],[20].

## 2.4 Transcripts analysis

mRNAs were extracted from 20 mg of muscle biopsy and prepared as described in [[15]]. 2 $\mu$g of RNA was reverse-transcribed with Invitrogen Superscript II reverse transcriptase. For conventional analysis, we performed overlapping RT-PCR reactions covering regions with *TTN* variants (supplementary table 1). For RNAseq analyses, sequencing was performed by IntegraGen SA (Evry, France) using the same protocol with poly-A selection of mRNA (Illumina (San Diego, CA, USA) TruSeq® Stranded Total RNA Library Prep) used in the GTEx sequencing project [[21]]. Paired-end 75-bp sequencing was performed on Illumina NovaSeq6000® platform as described in [[21]]. 88 Millions of reads were generated by RNAseq, including 687000 reads for *TTN* transcripts. RNA sequences alignment was performed using Ultrafast universal RNA-seq aligner (STAR) software [[22]] and analyzed using Integrative Genomics Viewer (IGV) [[23]] targeted on titin transcripts. The mean depth of RNA sequencing was 131 reads for titin transcripts NM_133378 corresponding to N2A isoform. Four exons had coverage under 30×: exon 11 (7×), exon 149 (14×), exon 150 (20×), and exon 151 (15×). These exons were described in [[19]] to be constitutively splice out for exon 11 and included in 35%, 34% and 40% of transcripts for exons 149, 150, 151 respectively. Exon 1 had a depth of sequencing of 157×, confirming that the 5' extremity was well covered

Protein solubilization from muscle biopsies was prepared as previously described [[24]]. For full length titin WB, 5 $\mu$l of protein extract were loaded on a SDS-Agarose 0.8% gel prepared as previously described [[25],[26] and ran for 3h20 at 15mA. Protein transfer on PVDF membrane was performed using wet transfer Trans blot® cell Bio-Rad (Bio-Rad, Hercules, CA, USA) at 400mA for 3h. Membranes were subsequently incubated in Odyssey® blocking buffer, washed and incubated overnight at 4 °C in Odyssey® blocking buffer in PBS specific primary antibodies: anti-titin specific for the C-terminal part M10-1 (Rabbit; 1:1000; kindly provided by Dr Isabelle Richard [[7]]) or N-terminal part (Mouse; 1:1000; Sigma SAB1400284). Membranes were washed and incubated for one hour with donkey anti-mouse IR Dye® 800CW (1:30,000) or donkey anti-rabbit IR Dye®680RD (1:30,000). Membranes were then washed, dried and scanned with the Odyssey® Infrared Imaging system.

For C-terminal part of titin WB, SDS-acrylamide 10% gel was used as previously described [[7]]. Anti-titin antibody M10-1, specific for the C-terminal part, was used at 1/500 followed by horseradish peroxidase–conjugated secondary antibodies (goat anti-rabbit sc2004, 1/20000, Santa Cruz) and enhanced chemiluminescence detection using the Substrat HRP Immobilon Western (Millipore-WBKLS0500).

# 3. Results

## 3.1 Clinical and imaging findings

Clinical features of all the patients are summarized in Table 1.

**Table 1 Summary of clinical findings of the patients.**

| | P1–P2 | P3 | P4 |
|---|---|---|---|
| Age | Twin sisters, 7 years old | 18 year | 55 year |
| Genetic variations | c.105036C>A p.(Tyr35012*) c.106531G>C p.(Ala35511Pro) | c.26503 A>T p.(Lys8835*) c.51437-4_51444delTCAGAACCCCCT | c.-14+5G>C c.68029A>G; p.(Thr22677Ala) c.65575+2T>G |
| Age of onset | <1 year | 3 year | 2 year |
| Neonatal features | Not | Unknown (adopted child) | Not |
| Early motor development | Axial hypotonia (6 months) Delayed walking (29 months) | Normal | Delayed walking (24 months) |
| | Moderate | | Initially, mild proximal weakness, with slow |

N.D: Not Done.

Open table in a new tab

Patients 1 and 2 (P1, P2) were twin sisters born to a non-consanguineous family. Pregnancy and delivery were normal, no neonatal hypotonia was reported. At the age of six months, they developed axial hypotonia. The motor development was delayed, and they were not able to walk before the age of 29 months. Neurological examination at the age of 4 years showed facial weakness, high arched palate, and mild proximal and axial weakness with Gowers's sign. There was no ptosis or ophthalmoparesis. Cardiological test at 9 years showed for P2 an ejection fraction at the lower limit

Creatin kinase (CK) level was normal and electromyography showed myopathic pattern. In patient 1, WB studies with an antibody against calpain-3 revealed reduced protein level (data not shown). *CAPN3* screening was normal. Brain MRI disclosed the presence of moderate periventricular white matter hyperintensity on Flair weighted signal (Fig. 1(A)). Muscular MRI was not done.

**Fig. 1 Clinical and magnetic resonance imaging (MRI) findings. (A) and (B) Flair weighted signal: Mild periventricular white matter hyperintensity in P2 and P3. (C) Axial T1 weighted signal, bilateral atrophy and fatty replacement in soleus and gastrocnemius muscles, right tibialis anterior and peroneus. Tight muscles were not involved.**

View Large Image | Download Hi-res image | Download (PPT)

Patient 3 (P3) is an adopted child from Latvia. At 3 years, parents noticed a waddling gait and difficulties in sport activities. Clinical examination at 8 years revealed facial weakness, moderate *scapula alata* and mild proximal weakness. There were no contractures or skeletal deformities. Cardiac assessment at 14 years was normal. There was a severe restrictive respiratory syndrome with Forced Vital Capacity (FVC) at 1.2L (33.2% of predicted). As for P1, brain MRI revealed the presence of moderate periventricular white matter hyperintensity on Flair weighted signal (Fig. 1(B))

Patient 4 (P4) is a sporadic case. The girl developed, from the age of 4 years, slowly progressive lower limb weakness. The patient progressively lost ambulation and was wheelchair bound at 17 years. Neurological examination at 45 years showed bilateral facial weakness, severe axial and proximal weakness of four limbs without contractures. Mild distal weakness was also present. There was restrictive respiratory syndrome with an FVC at 58%. At 55 years, a mild dilated cardiomyopathy with ejection fraction of 45% was revealed by cardiac ultrasonography. Muscle MRI of lower limbs showed bilateral soleus, lateral peroneus and tibial anterior involvement.

## 3.2 Muscle morphological data

A skeletal muscle biopsy was obtained from all patients except P2. There was an important percentage of centralized nuclei, from 9% in P1 to 95% in P4 (Fig. 2(A) and (B)) and minicore-like lesions with NADH oxidative reaction (Fig. 2(C)–(E)). P1, P2, P3 and P4 were diagnosed as having a centronuclear myopathy. Ultrastructural studies in P3 and P4 revealed the presence of multifocal

**Fig. 2 Histopathological and ultrastructure (EM) characteristics of patients' skeletal muscles. (A) and (B) H&E coloration of P1 and P4: multiple muscular fibers with internal and centralized nuclei. (C)–(E) NADH staining show multifocal areas with reduction of staining compatible with minicores in patients P1, P3, P4. (F)–(H) Ultrastructure analyses by electron microscopy of P4. (F) Well-delimited cap structure filled with thin filaments, sarcomeres fragments and cellular debris. (G) Left part, focal and large area of myofibrillar disorganization with Z-line streaming and absence of mitochondria corresponding to a minicore and confirmed pale areas in NADH staining. Right part, Centralized nucleus. (H) Small and clear sarcomere disorganization areas with Z-line material accumulation.**

View Large Image | Download Hi-res image | Download (PPT)

As a whole, excessive internal nuclei, minicore-like and cap structures were consistent with *TTN* related muscle morphological presentation.

## 3.3 Molecular and protein results

Localization of variants on corresponding titin domains is shown on Fig. 3. The exon numbering is reported following the numbering used in LOVD. No other pathogenic variants than the *TTN* ones were identified in the reported patients.

**Fig. 3 Schematic localization of patient mutations on titin. Description of the principal domains of titin protein composed by the Z-disk in N-terminal part of the protein to the M-band in C-terminal. Between these two domains, titin is composed by the I-band, Ig-like motif rich, the PEVK domain rich in Proline (P), Glutamic acid (E), Valine (V) and Lysine (K) amino acids repeats, the A-band rich in Ig-like and Fibronectin type III motifs. Each domain interacts with some of proteins partners essential for development, maintenance and integrity of the sarcomere. Localization of patient mutations identified by NGS and verified by Sanger sequencing are described in green for P1 and P2 in red for P3 and in blue for P4.**

View Large Image | Download Hi-res image | Download (PPT)

### 3.3.1 P1 and P2 patients

P1 and P2 have two variants, a nonsense variant in exon 359, c.105036C>A p.(Tyr35012*) inherited from the mother and a missense variant in exon 360, c.106531G>C p.(Ala35511Pro) from the father, both absent from gnomAD population database. Patients do not have other siblings to enlarge the segregation study. The variants are both localized in the genomic region encoding the M-band domain of titin (Fig. 3). The missense variant in exon 360 affects the last nucleotide of the exon and is predicted to have an impact on exon 360 RNA splicing (HSF score shift at –46,1% and MaxEnt score at-29%). To confirm this prediction, we investigated the region of transcripts containing the variant (exons 359-362) by RT-PCR and Sanger sequencing (Fig. 4(A)). cDNA agarose gel revealed the presence of two bands of intensity difference, and sequencing of RT-PCR products identified two populations of transcripts, a major one with aberrant splicing (exon 360 skipping) and a minor one with normal splicing of exon 360. This minor transcript with normal exon 360 splicing do not carry the paternal c.106531G>C variant in exon 360, indicating that the paternal variant results in 100% of the transcripts with the exon 360 skipping. This experiment also suggests that the transcripts with the maternal nonsense variant have a reduced level, probably due to RNA degradation by Nonsense Mediated RNA Decay (NMD). Exon 360 skipping disrupts the open reading, leading to a Stop codon 6 nucleotides downstream from the frameshift. Overall, both *TTN* mutated alleles in P1 and P2 are predicted to produce a M-band truncated protein (Fig. 5(A)). WB analysis of the C-terminal part of titin showed the loss of the C-term p45 band in P1 and, thereby, the loss of titin C-terminal portion (Fig. 5(B)). The total absence of the C-terminal fragments is a further argument suggesting that no normal transcripts are produced from the paternal allele with the variant affecting the last nucleotide of the exon.


**Fig. 4 Titin transcripts analyses. (A) gDNA and cDNA analyses of P1 c.106531G>C variant. gDNA Sanger sequence of the c.106531G>C in exon 360 is shown. cDNA analyses showed an impact on splicing. Agarose gel of cDNA shows two bands, a faint one at the normal size (3,8MDa) and a second smaller molecular weight one corresponding to the exon 360 skipping allele that disrupt the open reading frame. (B) gDNA and cDNA analyses schemes for P3 titin transcripts. The exon 273 c.51437-4_514444delTCAGAACCCCCT variant deletes the natural acceptor splice site and leads to the use of a cryptic acceptor splice site 21 bases downstream, represented by a blue arrow. This deleted transcript is in frame and is predicted to result to the lack of seven amino acids at the beginning of exon 274 in frame. (C) cDNA study by RT-PCR sequencing of P4 titin transcripts containing the c.65575+2T>G mutation. Three populations of transcripts were visible on agarose gel in P4. Black arrow corresponds to the WT allele, green arrow to the complete skipping of exon 313 (306 nucleotides loss), red**

**represented the coverage of each sequence. The crescents represent the splice junctions identified in the control (blue crescents) and the P4 patient (red crescents) transcripts, with the number of reads indicated above. In P4, the same three transcript populations identified by RT-PCR Sanger sequencing were also detected: one normal splice pattern between exons 312 and 314 (similar to the healthy control), a transcript with complete skip of exon 313 and another one with the use of the cryptic donor splice site in exon 313.**

View Large Image | Download Hi-res image | Download (PPT)

**Fig. 5 Titin protein analyses. (A) Patients 1 and 2, predicted titin alleles. Both mutated alleles are predicted to produce a C-terminal truncated protein, of 3,5 and 3,6 MDa respectively. (B) Control (Ctrl) and P1, titin C-term skeletal muscle immunoblot. M-line titin samples were analyzed by immunoblotting using an anti-TITIN C-term (M10.1). In control, muscle proteins extract from healthy patient (AFM-Myobank), Rb positive control patient with C-term truncated variants (published in De Cid et al., 2015 [[8]]) and P1 with absence of p45 peptide specific of C-term part of titin as a consequence of the two M-band truncated variants. Black star is unspecific band. Loading was normalized with GAPDH antibody. (C) Scheme of P4 predicted titin alleles. In addition to the 3.8MDa predicted titin allele with the missense variant p.(Thr22677Ala), the in frame transcript with exon 313 skipping due to c.65575+2T>G is predicted to lead to a 3.79 MDa titin, indistinguishable from the normal length titin. The out of frame transcript population missing the last 163 bases of exon 313 is predicted to produce a C-term truncated protein with an approximately molecular weight of 2,2MDa. (D) Control (Ctrl) and P4 skeletal muscle titin WB analysis on SDS-Agarose gel with specific antibodies against C-term part (M10.1) and N-term part (Sigma SAB1400284). C-term antibody allows to observe N2A isoform (3,8MDa) and T2 titin degradation products (around 3MDa). N-term antibody analysis revealed the presence of normal N2A protein (3,8MDa) and Novex-3 (around 1MDa) in Ctrl and P4 muscles. This antibody shows several bands in the Ctrl muscle, and only one additional band in P4 muscle with a molecular weight of 2,2MDa. This band could correspond to the truncated protein due to the specific characterized splicing effect in exon 313.**

View Large Image | Download Hi-res image | Download (PPT)

### 3.3.2 P3 patient

In P3, two heterozygous *TTN* variants, located in exon 93, c.26503 A>T p.(Lys8835*) and in intron 272-exon 273, c.51437-4_51444delTCAGAACCCCCT, were identified. In the absence of possible sampling of his parents (adopted child), the phasing of the variants could not be determined. They

first 8 nucleotides of exon 273. The latter is predicted to affect exon 273 splicing (HSF and MaxEnt prediction scores for loss of exon 273 splicing: 100%). RT-PCR and cDNA sequencing of the region containing the deletion (exons 272–276) identified aberrant transcripts with a loss of the 21 first nucleotides of exon 273, due to the use of a cryptic acceptor splice site 13 bp downstream the genomic deletion (Fig. 4(B)). This deleted transcript population is not predicted to affect the reading frame but rather to lead to an internally deleted protein, lacking seven amino acids encoded by exon 273 (Fig. 4(B)). These seven amino acids are located in Fibronectin type-III 24, a myosin interaction domain. Titin WB was not performed for this patient due to the lack of biopsy material.

#### 3.3.3 P4 patient

P4 has three *TTN* variants, c.-14+5G>C in exon 1 and c.68029A>G; p.(Thr22677Ala) in exon 321, both absent in her mother (no sample was provided for the father) and c.65575+2T>G in intron 313 inherited from the mother. There was no proband's siblings to complete the segregation study. All these variants were absent from gnomAD population database. Exon 1 is reported to be expressed but not translated into amino acids. Presumably on the same allele, the missense mutation in exon 321, p.(Thr22677Ala), is localized in A band, Fibronectin type-II 64 domain. It has an MPA score at 6.7/10 and is predicted to destabilize the protein structure, according to titindb. cDNA analyses of the region containing the c.68029A>G; p.(Thr22677Ala) variant showed normal splicing and normal allelic balance with the maternal allele, not supportive of a potential reduction of *TTN* expression caused by the exon 1 variant presumably *in cis*. On the other allele, the c.65575+2T>G variant is predicted to have an impact on exon 313 splicing (HSF and MaxEnt predictions scores: 100%). This was confirmed by RT-PCR sequencing and RNAseq that revealed a complex effect with two abnormal populations of transcripts (Fig. 4(C) and (D)). A full exon 313 skipping (306 nucleotides) was found in one of the transcript population, leading to the synthesis of an internally deleted protein lacking 102 residues in A-band, in a myosin interaction domain [[27]]. This deletion is extremely small compared to the size of the protein and is therefore not detectable in WB. In the second population, transcripts are deleted of the 163 last nucleotides of exon 313, due to the use of a cryptic donor splice site (GTACGG) within this exon. This transcript population induces a shift in the reading frame and a Stop codon 12 nucleotides downstream from the shift. If not degraded by nonsense mediated RNA decay (NMD), this allele is predicted to produce a truncated protein with an approximate molecular weight of 2.2MDa (Fig. 5(C)), lacking a large part of the A-band and the M-band. RNA-seq analyses allowed to exclude elusive variants such as deep intronic variants affecting splicing. WB analysis of muscle biopsy showed the presence of normal N2A protein (3.8MDa) and one additional band (although at a low amount) at an approximate molecular weight

truncated protein due to the premature stop codon in transcripts induced by the splicing defect in exon 313.

## 4. Discussion

Due to the widespread use of NGS, *TTN* is emerging as a major causative gene of neuromuscular disorders. Interpretation of the pathogenic effect of variants is particularly challenging. In this study we present an exhaustive workflow in order to confirm the pathogenicity of *TTN* variants in four patients with recessive congenital myopathy with centralized nuclei, minicores and Cap structures.

With respect to the phenotype of the patients, the presence of mild diffuse weakness, facial weakness and respiratory insufficiency was concordant with titinopathies phenotypic spectrum [[5], [14]. In a recent series of 30 titin patients, most of them had mild to moderate weakness (81%), facial weakness (70%) and respiratory insufficiency (63%) [[14]]. Although not specific of titinopathies, some signs were previously reported on congenital myopathy patients suspected of titinopathies [[14]]. In Oates et al., study (2018), 19 of 26 patients had high arched palate, one of 22 had pes cavus and 3 of 12 patients had minor structural abnormalities of unknown significance on brain MRI. This sign could be better explored in the future.

Cardiomyopathy was also a frequent feature found in 46% of cases [[14]]. Of note, P4 developed dilated cardiomyopathy at 50 years and P2 had ejection fraction at the lower limit of the normal range. Our study confirms that a strict cardiac workup should be performed in all congenital titinopathy patients as subtle cardiac involvement might be present in infancy and an overt cardiomyopathy might develop later in life.

From a myopathologic standpoint, all patients presented centralized nuclei and minicore-like lesions. Our findings are in line with data reported by us and others [[13],[14], where the presence of prominent nuclear centralizations and alterations in the intermyofibrillar network are prominent features of congenital titinopathies.

With respect to the interpretation of genetic variants in *TTN*, Savarese and colleagues have proposed that identifying two *TTN* truncating variants in *trans* plus a suggestive phenotype results in a diagnosis of titinopathy, but a complete molecular characterization of variants affecting the canonical or noncanonical splice sites by cDNA or protein studies was suggested. [[3]]. In our

out-of-frame exon 360 skipping in 100% of the transcripts. Both *TTN* variants lead to a M-band truncation. In line with the current understanding, and considering that the total absence of titin is most probably incompatible with life [[28],[29], we expect both the mutated alleles to result in a truncated protein. Of interest, WB showed calpain-3 clear reduction consistent with previous reports of calpain 3 deficiency secondary to truncation of the titin C-terminal part [[7],[8].

P3 has a nonsense variant in exon 93 in the I-band domain and a splicing variant resulting in a small internal inframe deletion in exon 273. Considering the current understanding, the nonsense variant in the I-band most probably causes a NMD and is unlikely to result in a truncated protein. The aberrant transcripts resulting from the splicing variant lacks the 21 first nucleotides of exon 273, leading to the loss of seven residues within a titin-myosin interaction domain. Since phasing with the nonsense variant is impossible, and the effect of the splicing variant is not an out-of-phase truncation, this splice variant is then considered as probably pathogenic and P3 is most probably a titinopathy case.

For P4, the interpretation is still challenging. He harbors a missense in exon 321 and a splice variant in intron 313. Transcript analyses showed complex consequences of the splice variant in intron 313, with a population of transcripts harboring an in-frame complete exon 313 skipping associated with another population of out-of-frame transcripts resulting from activation of a cryptic splice site. If not degraded by NMD, the latter is predicted to lead to a truncated protein of an approximate molecular weight of 2.2MDa lacking a large part of the A-band and the M-band. One additional band of 2.2 Mb was detected by WB analysis on the P4 muscle. Even if the correspondence of this band with the truncated protein due to the characterized splicing defect is not certain, this observation suggests that the transcript with the premature stop codon in exon 313 would not be degraded by nonsense mediated decay. Missense variants interpretation is a real challenge and need the association of deep clinical, histopathological and radiological phenotyping, complete molecular analyses including large segregation studies, and functional studies. Our study has limitation since the presence of clinical and histological features consistent with a congenital titinopathy cannot be a stand-alone proof. We could not perform segregation studies nor functional analyses for the missense variant identified in P4, that is then considered as uncertain significance according to ACMG guidelines. With the confirmation of paternal allele inheritance, the missense variant for P4 would have been classified as “likely pathogenic”, underlining the importance of segregation studies. In their proposed workflow to interpret monoallelic *TTN* variants pathogenicity in congenital myopathies, Savarese et al. [[10]] also recommend to search for the presence of a further elusive truncating variant. No such variant was identified in P4 by RNAseq analysis. Even if the phenotype is in agreement, and the

should be considered as a “possible titinopathy case”. Functional studies and/or identification of other cases with the same variant would be important to confirm pathogenic effects of the missense variant. This challenging case highlights the importance of sharing data using curated databases such as LOVD and publication reports using the same comprehensive approach [[14],[30].”

In conclusion, our study illustrates that deep clinical and muscle morphologic phenotyping together with segregation studies, transcripts and protein analyses are essential for the interpretation of titin variants. Analysis of the consequences on transcripts of all variants is crucial, in order to have an exhaustive understanding of their effects at the transcriptional and protein levels. Given the complexity of titin transcripts in healthy subjects and patients, RNASeq will be the technique of choice as it allows to identify *TTN* variants consequences on all the length of all transcript's isoforms. This study and many others [[14],[30] are essential to describe such challenging cases in publications using this approach. The next steps will include the study of protein dysfunction at the structural or interacting levels, since published studies suggest that some titin variants could affect the stability of the protein and its interaction with direct binding partners [[3],[5],[31].

## Acknowledgments

The authors thank Myobank-AFM for providing control muscle biopsies, Isabelle Richard for titin antibody provided and the French Titin Consortium for all the discussion about patient suspected of titinopathies.

## Study funding

This work was funded by AFM 21384 grant (The French Muscular Dystrophy Association (AFM-Téléthon)), the Délégation à la Recherche Clinique et à l'Innovation du Groupement de Coopération Sanitaire de la Mission d'Enseignement, de Recherche, de Référence et d'Innovation (DRCI-GCS-MERRI) de Montpellier-Nîmes and the French Foundation for Rare Diseases (FFRD) under the program « High throughput sequencing and rare diseases ».

# Appendix. Supplementary materials

Help with docx files

## References


1. Linke WA • Hamdani N.
**Gigantic business: titin properties and function through thick and thin.**
*Circ Res.* 2014; **114**: 1052-1068

View in Article
Scopus (189) • PubMed • Crossref • Google Scholar

2. Akinrinade O • Koskenvuo JW • Alastalo TP
**Prevalence of titin truncating variants in general population.**
*PLoS One.* 2015; **10**e0145284

View in Article
Scopus (55) • PubMed • Crossref • Google Scholar

3. Savarese M • Maggi L • Vihola A • Jonson PH • Tasca G • Ruggiero L • et al.
**Interpreting genetic variants in titin in patients with muscle disorders.**
*JAMA Neurol.* 2018; **75**: 557-565

View in Article
Scopus (32) • PubMed • Crossref • Google Scholar

4. Chauveau C • Rowell J • Ferreiro A
**A rising titan: TTN review and mutation update.**
*Hum Mutat.* 2014; **35**: 1046-1059

View in Article
Scopus (124) • PubMed • Crossref • Google Scholar

**Recessive truncating titin gene, TTN, mutations presenting as centronuclear myopathy.**
*Neurology.* 2013; **81**: 1205-1214

View in Article
Scopus (122) • PubMed • Crossref • Google Scholar

6. Chauveau C • Bonnemann CG • Julien C • Kho AL • Marks H • Talim B • et al.
**Recessive TTN truncating mutations define novel forms of core myopathy with heart disease.**
*Hum Mol Genet.* 2014; **23**: 980-991

View in Article
Scopus (98) • PubMed • Crossref • Google Scholar

7. Evilä A • Vihola A • Sarparanta J • Raheem O • Palmio J • Sandell S • et al.
**Atypical phenotypes in titinopathies explained by second titin mutations.**
*Ann Neurol.* 2014; **75**: 230-240

View in Article
Scopus (49) • PubMed • Crossref • Google Scholar

8. De Cid R • Ben Yaou R • Roudaut C • Charton K • Baulande S • Leturcq F • et al.
**A new titinopathy: childhood-juvenile onset Emery-Dreifuss-like phenotype without cardiomyopathy.**
*Neurology.* 2015; **85**: 2126-2135

View in Article
Scopus (26) • PubMed • Crossref • Google Scholar

9. Hackman P • Vihola A • Haravuori H • Marchand S • Sarparanta J • De Seze J • et al.
**Tibial muscular dystrophy is a titinopathy caused by mutations in TTN, the gene encoding the giant skeletal-muscle protein titin.**
*Am J Hum Genet.* 2002; **71**: 492-500

10. Savarese M • Johari M • Johnson K • Arumilli M • Torella A • Töpf A • et al.
**Improved criteria for the classification of titin variants in inherited skeletal myopathies.**
*J Neuromuscul Dis.* 2020; **7**: 153-166

View in Article
Scopus (8) • PubMed • Crossref • Google Scholar

11. Ávila-Polo R • Malfatti E • Lornage X • Cheraud C • Nelson I • Nectoux J • et al.
**Loss of sarcomeric scaffolding as a common baseline histopathologic lesion in titin-related myopathies.**
*J Neuropathol Exp Neurol.* 2018; **77**: 1101-1114

View in Article
Scopus (10) • PubMed • Crossref • Google Scholar

12. Carlier R-Y • Quijano-Roy S.
**Myoimaging in congenital myopathies.**
*Semin Pediatr Neurol.* 2019; **29**: 30-43

View in Article
Scopus (9) • PubMed • Crossref • Google Scholar

13. Hackman P • Udd B • Bönnemann CG • Ferreiro A • Udd B • Hackman P • et al.
**219th ENMC International Workshop Titinopathies International database of titin mutations and phenotypes, Heemskerk, The Netherlands, 29 April–1 May 2016.**
*Neuromuscul Disord.* 2017; **27**: 396-407

View in Article
Scopus (21) • PubMed • Abstract • Full Text • Full Text PDF • Google Scholar

14. Oates EC • Jones KJ • Donkervoort S • Charlton A • Brammah S • Smith JE • et al.
**Congenital titinopathy: comprehensive characterization and pathogenic insights.**
*Ann Neurol.* 2018; **83**: 1105-1124

15. Zenagui R • Lacourt D • Pegeot H • Yauy K • Morales RJ • Theze C • et al.
**A reliable targeted next-generation sequencing strategy for diagnosis of myopathies and muscular dystrophies, especially for the giant titin and nebulin genes.**
*J Mol Diagn.* 2018; (Published Online First)
https://doi.org/10.1016/j.jmoldx.2018.04.001

View in Article
Scopus (18) • PubMed • Abstract • Full Text • Full Text PDF • Google Scholar

16. Richards S • Aziz N • Bale S • Bick D • Das S • Gastier-Foster J • et al.
**Standards and guidelines for the interpretation of sequence variants: a joint consensus recommendation of the American College of medical genetics and genomics and the association for molecular pathology.**
*Genet Med.* 2015; **17**: 405-424

View in Article
Scopus (9689) • PubMed • Crossref • Google Scholar

17. Yauy K • Baux D • Pegeot H • Van Goethem C • Mathieu C • Guignard T • et al.
**MoBiDiC prioritization algorithm, a free, accessible, and efficient pipeline for single-nucleotide variant annotation and prioritization for next-generation sequencing routine molecular diagnosis.**
*J Mol Diagnostics.* 2018; **20**: 465-473

View in Article
Scopus (8) • PubMed • Abstract • Full Text • Full Text PDF • Google Scholar

18. Laddach A • Gautel M • Fraternali F
**TITINdb-a computational tool to assess titin's role as a disease gene.**
*Bioinformatics.* 2017; **33**: 3482-3485

View in Article
Scopus (20) • PubMed • Crossref • Google Scholar

**e complexity of titin splicing pattern in human adult skeletal muscles.**

*Skelet Muscle.* 2018; **8**: 11

View in Article

Scopus (23) • PubMed • Crossref • Google Scholar

20. Uro-Coste E • Fernandez C • Authier FJ • Bassez G • Butori C • Chapon F • et al.
**Management of muscle and nerve biopsies: expert guidelines from two French professional societies, Société française de neuropathologie and Société française de myologie and a patient-parent association, Association Française contre les myopathies.**
*Rev Neurol (Paris).* 2010; **166**: 477-485

View in Article

Scopus (10) • PubMed • Crossref • Google Scholar

21. Cummings BB • Marshall JL • Tukiainen T • Lek M • Donkervoort S • Foley AR • et al.
**Improving genetic diagnosis in Mendelian disease with transcriptome sequencing.**
*bioRxiv.* 2017; **5209**074153

View in Article

Google Scholar

22. Dobin A • Davis CA • Schlesinger F • Drenkow J • Zaleski C • Jha S • et al.
**STAR: ultrafast universal RNA-seq aligner.**
*Bioinformatics.* 2013; **29**: 15-21

View in Article

Scopus (12731) • PubMed • Crossref • Google Scholar

23. Thorvaldsdóttir H • Robinson JT • Mesirov JP
**Integrative Genomics Viewer (IGV): high-performance genomics data visualization and exploration.**
*Brief Bioinform.* 2013; **14**: 178-192

View in Article

24. Hudson B • Hidalgo C • Saripalli C • Granzier H
**Hyperphosphorylation of mouse cardiac titin contributes to transverse aortic constriction-induced diastolic dysfunction.**
*Circ Res.* 2011; **109**: 858-866

View in Article
Scopus (48) • PubMed • Crossref • Google Scholar

25. Perrin A • Metay C • Villanova M • Carlier R • Pegoraro E • Juntas Morales R • et al.
**A new congenital multicore titinopathy associated with fast myosin heavy chain deficiency.**
*Ann Clin Transl Neurol.* 2020; : 1-9

View in Article
Google Scholar

26. Greaser ML • Warren CM.
**Electrophoretic separation of very large molecular weight proteins in SDS agarose.**
*Methods Mol Biol.* 2019; **1855**: 203-210

View in Article
Scopus (2) • PubMed • Crossref • Google Scholar

27. Kontrogianni-Konstantopoulos A • Ackermann MA • Bowman AL • Yap S.V. • Bloch RJ
**Muscle giants: molecular scaffolds in sarcomerogenesis.**
*Physiol Rev.* 2009; **89**: 1217-1267

View in Article
Scopus (166) • PubMed • Crossref • Google Scholar

28. Gerull B • Gramlich M • Atherton J • McNabb M • Trombitás K • Sasse-Klaassen S • et al.
**Mutations of TTN, encoding the giant muscle filament titin, cause familial dilated rdiomyopathy.**
*t Genet.* 2002; **30**: 201-204

View in Article

Scopus (410) • PubMed • Crossref • Google Scholar

29. Weinert S • Bergmann N • Luo X • Erdmann B • Gotthardt M
**M line-deficient titin causes cardiac lethality through impaired maturation of the sarcomere.**
*J Cell Biol.* 2006; **173**: 559-570

View in Article

Scopus (78) • PubMed • Crossref • Google Scholar

30. Savarese M • Vihola A • Oates EC • Barresi R • Fiorillo C • Tasca G • et al.
**Genotype-phenotype correlations in recessive titinopathies.**
*Genet Med.* 2020; **0**
https://doi.org/10.1038/s41436-020-0914-2

View in Article

Scopus (6) • Crossref • Google Scholar

31. Rossi D • Palmio J • Evilä A • Galli L • Barone V • Caldwell TA • et al.
**A novel FLNC frameshift and an OBSCN variant in a family with distal muscular dystrophy.**
*PLoS One.* 2017; **12**: 1-21

View in Article

Scopus (22) • Crossref • Google Scholar

# Article Info

## Publication History

Published online: September 28, 2020

Accepted: September 23, 2020

ed in revised form: August 26, 2020

ed: May 7, 2020

## Identification

DOI: https://doi.org/10.1016/j.nmd.2020.09.032



# Figures

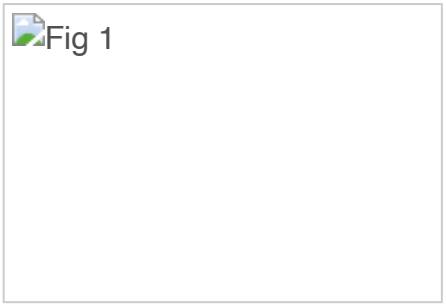


**Fig. 1** Clinical and magneti…

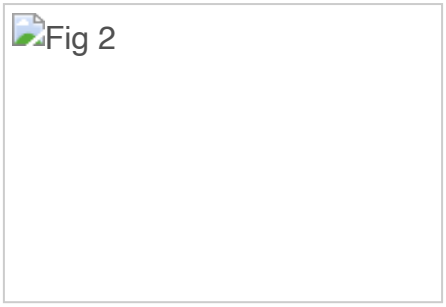


**Fig. 2** Histopathological an…

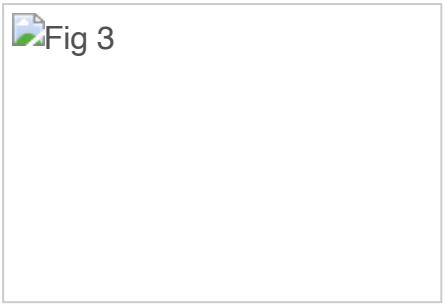


**Fig. 3** Schematic localizatio…

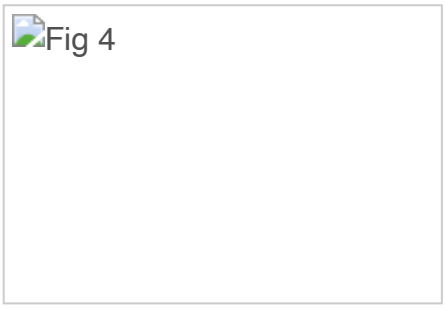


**Fig. 4** Titin transcripts analy…

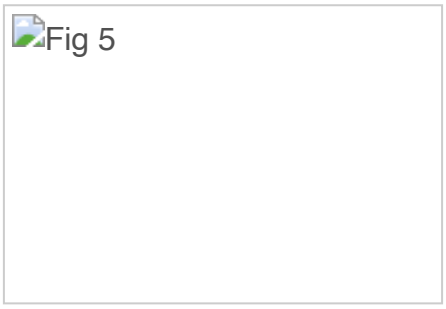


**Fig. 5** Titin protein analyses…

**es**

**Table 1 :** Summary of clinical findings of the patients.

## Related Articles